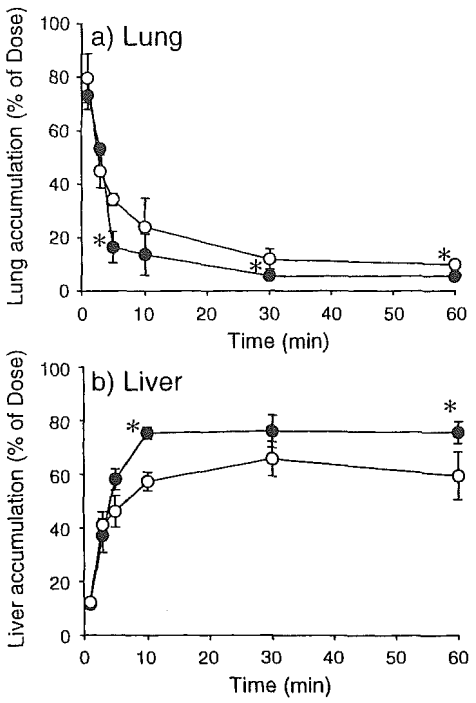

Fig. 4. In vivo biodistribution of ^{32}P-labeled DNA complexed with Man/DOPE (●) and Man/DOPC (○) liposomes after intravenous injection into mice. DNA (50 μg) was complexed with cationic lipids at a charge ratio of 1.0:2.3 (−:+). Tissue accumulation was determined at each time-point. Each value represents the mean ± S.D. (n=3). Statistical analysis was performed by Student's t-test (* indicated $P<0.05$).

nous injection of Man/DOPE and Man/DOPC liposome/[^{32}P]pDNA complex. Both complexes accumulated in the lung while Man/DOPE liposome complex were eliminated more rapidly from the lung and accumulated significantly higher in the liver than the Man/DOPC liposome complexes. To evaluate the contribution of the mannose receptor-related mechanism to the liver accumulation of both mannosylated cationic liposome/pDNA complexes, the liver accumulation of both complexes was evaluated in mice pre-injected with 50 mg/kg mannosylated bovine serum albumin (Man-BSA), a ligand of the mannose receptor involved in the liver accumulation of mannosylated liposomes. Accumulation of Man/DOPE liposome complexes in the liver was significantly inhibited by pre-injection of Man-BSA, whereas that of Man/DOPC liposome complexes was unaffected (Fig. 5).

3.5. Transfection activities of mannosylated liposomes after intravenous and intraportal DNA transfection

To elucidate the role of DOPE in in vivo transfection, transfection activities of Man/DOPE and Man/DOPC liposome complex to major organs were evaluated 6 h after intravenous injection or intraportal administration of liposome/pDNA complexes into mice. As shown in Fig. 6, Man/DOPE liposome complexes showed a higher transfection activity in the liver and spleen than Man/DOPC liposome complexes following both intravenous and intraportal administration.

3.6. Intrahepatic gene expression properties after intravenous administration

We next investigated preference of Man liposome/pDNA complex to liver parenchymal cells (PC) and non-parenchymal cells (NPC). The distribution of expressed luciferase activity between the liver PC and NPC after intravenous administration of mannosylated cationic liposome/pDNA complexes is shown in Fig. 7. Gene expression of the Man/DOPE complex was preferentially observed in NPC and the activity

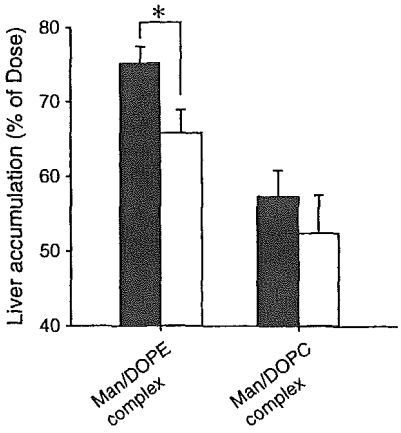

Fig. 5. Inhibition of liver accumulation of liposome/pDNA complexes after intravenous injection by co-administration with Man-BSA in mice. DNA (50 μg) was complexed with cationic lipids at a charge ratio of 1.0:2.3 (−:+). Tissue accumulation was determined at each time-point. Liposome/pDNA complexes were injected with (□) or without (■) Man-BSA. Each value represents the mean+S.D. (n=3). Statistical analysis was performed by Student's t-test (* indicated $P<0.05$).

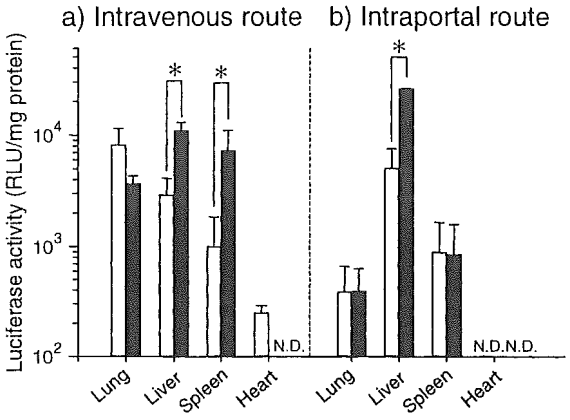

Fig. 6. Effect of administration route on the transfection activity of Man/DOPE (■) and Man/DOPC (□) liposomes/pDNA complexes. pDNA (50 μg) was complexed with cationic lipid at a charge ratio of 1.0:2.3 (−:+). Liposome/pDNA complexes were administrated to mice by the intravenous (i.v.) or intraportal (i.p.) route. Luciferase activity was determined 6 h post-injection in the lung, liver, spleen and heart. Each value represents the mean+S.D. ($n=3$). Statistical analysis was performed by Student's t-test (* indicated $P<0.05$).

ratio of NPC to PC on a cell-number basis was calculated to be 13.7. On the other hand, Man/DOPC liposomes gave an NPC/PC ratio of 2.13.

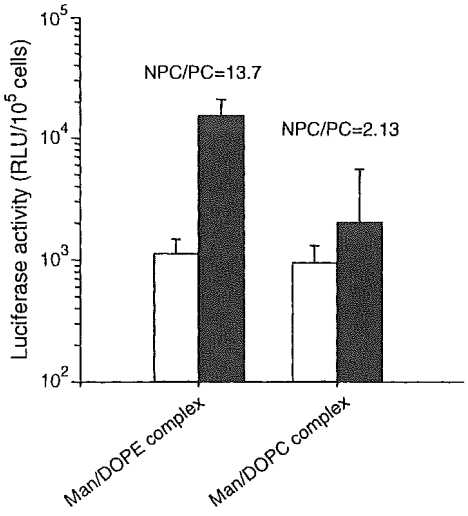

Fig. 7. Hepatic cellular localization of luciferase activity after intravenous administration of liposome/pDNA complexes in mice. pDNA (50 μg) was complexed with cationic lipid at a charge ratio of 1.0:2.3 (−:+). Liposome/pDNA complexes were administered to mice by intravenous (i.v.) injection. Luciferase activity was determined 6 h post-injection in the PC (□) and NPC (■). Each value represents the mean+S.D. ($n=3$).

3.7. Interaction with erythrocytes

To evaluate the effect of DOPE in interaction with red blood cells, that is known to affect transfection activity of cationic liposome, both complex were incubated with red blood cells suspension. After 10-min incubation with Man/DOPC liposome/pDNA complexes, no significant change was observed in the erythrocytes (Fig. 8a, b). In contrast, when the

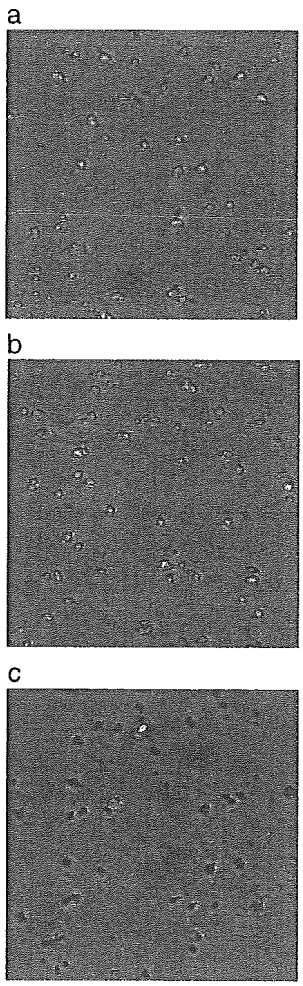

Fig. 8. Erythrocyte–erythrocyte fusion induced by the liposome/pDNA complexes. Six hundred microliters of erythrocyte suspension (hematocrit 0.1%) was incubated with 100 μl of the complexes (charge ratio=1.0:2.3 (−:+), 0.167 μg/μl) for 10 min. (a) Untreated erythrocytes, (b) erythrocytes incubated with Man/DOPC liposomes complexes, (c) erythrocytes incubated with Man/DOPE liposomes complexes.

erythrocytes were incubated with Man/DOPE liposome/pDNA complexes, fusion and aggregation between erythrocytes occurred (Fig. 8c).

4. Discussion

Since mannosylated cationic liposome/pDNA complexes are taken up by the macrophages via mannose receptor-mediated endocytosis and rapidly sorted from endosomes to lysosomes [13], it is very important to avoid degradation of pDNA in lysosomes as well as release into the cytoplasm in order to obtain effective gene transfection by Man liposomes. As shown in Figs. 1 and 2, DOPE containing Man liposomes showed a higher gene expression on cultured macrophages without enhancing cellular association. This phenomenon can be explained by the proposed mechanism that DOPE destabilizes the endosomal membrane and leads an accelerated release of DNA into the cytosol [14–17]. Thus, DOPE in the Man liposomes could act as a functional lipid to improve the intracellular fate of pDNA. In this study, we have shown that Man liposomes containing DOPE complex also showed higher gene expression in the liver after intraportal administration (Fig. 6). This result suggests that DOPE in Man liposomes could act even under in vivo conditions. As far as conventional cationic liposome/pDNA complex, many studies including ours have shown that DOPE containing cationic liposome showed limited gene expression after intravenous administration because of the instability of the complex in the blood compartment [18–20]. One possible explanation of this discrepancy is transfection to the target cells. Our previous report demonstrated that glycosylated proteins and liposome/pDNA complexes are internalized faster than cationic proteins and liposome/pDNA complexes, which are internalized by the liver via adsorptive endocytosis [21]. This suggests that Man liposome complexes could be internalized to a greater extent than conventional cationic liposome complexes, resulting in reduced degradation outside the target tissue. These results from this study suggest that DOPE could enhance gene expression in the target tissue through intracellular sorting in the target tissue. In our previous study, we have shown that Man liposome/pDNA complexes were rapidly sorting from endosomes to lysosomes. Taking these findings into consideration, further modulation of intracellular sorting with some functional device should lead to more efficient gene expression in the macrophages. So far, functional materials such as influenza virus hemagglutinin subunit HA-2 (mHA2) [22], fusigenic peptide, and polyhistidine [23] have been grafted to the vectors to improve the intracellular sorting of cationic carrier/pDNA complexes. Modulation by grafting such functional molecules might be effective in the further development of mannosylated cationic liposomes.

For efficient targeted gene delivery, accessibility of cationic liposome/pDNA complexes to the target site is also essential. After administration into the blood circulation, the pDNA complexes interact with various cells and molecules, such as serum proteins [19] and erythrocytes [18,24,25] because the cationic nature of the complexes attracts negatively charged cells and molecules, which eventually leads to an alteration in the physicochemical properties of the complexes. Many studies, including our own, have demonstrated that cationic liposome/pDNA complexes accumulate in the lung, which is the first-pass organ and the highest gene expression is shown in lung. This accumulation in the lung is considered to be a barrier to cationic liposome-mediated targeted gene delivery to the liver. As shown in Fig. 4, [^{32}P]-labeled Man/DOPE liposome/pDNA complexes were eliminated more rapidly from the lung than [^{32}P]-labeled Man/DOPC liposome/pDNA complexes. This phenomenon is partly consistent with the observation by Liu et al. that DOPE-containing cationic liposomes are more rapidly eliminated from the lung than cholesterol-containing cationic liposomes after intravenous administration [19]. Furthermore, [^{32}P]-labeled Man/DOPE liposome/pDNA complexes accumulate to a higher degree in the liver than Man/DOPC liposome/pDNA complexes in a mannose receptor-dependent manner. These results suggest that DOPE containing Man liposomes could achieve more efficient gene expression in the target site than Man/DOPC liposomes. In fact, Man liposomes containing DOPE show a higher degree of gene expression in the liver than Man/DOPC liposome/pDNA complexes and their gene expression is highly selective for the liver NPC, whereas Man/DOPC liposome/pDNA complexes do not (Figs. 6 and 7). This is partly

consistent with our previous report showing that Man liposomes based on DOTMA and cholesterol, known to accumulate in the lung, did not enhance gene expression in the liver [11]. These observations suggest that rapid elimination from the lung might also be important.

In this study, Man/DOPC liposome complexes did not show any receptor-mediated uptake by the liver (Fig. 5). One possible explanation of this phenomenon might be accessibility of complex to target site and state of complex under in vivo condition. Present study revealed that Man/DOPE liposome complexes seem to be unstable in erythrocytes than Man/DOPC liposome complexes (Fig. 8), whereas intravenously injected Man/DOPE liposome complexes was eliminated from the lung more rapidly than Man/DOPC liposome complexes (Fig. 4). It has been reported that endogenous components including erythrocyte and serum disintegrates cationic liposome/pDNA complexes after intravenous injection [18,33]. Therefore, it is speculated that this rapid elimination of Man/DOPE liposome complexes from the lung allow Man/DOPE liposome complexes to access NPCs without losing transfection activity to some extent, but Man/DOPC liposome complexes lost transfection activity (including the recognition by mannose receptor) due to long retention in the lung. Although some studies have demonstrated that lipid composition in the cationic liposomes affects pharmacokinetics of interaction between cationic liposome/pDNA complexes and blood components [18,19,24], there has been little information in pharmacokinetics of interaction with endogenous and complex in the targeted gene delivery. Further studies are needed to clarify the interaction with endogenous components with Man liposome complexes for improvement in the transfection efficiency in the liver NPCs.

Sakurai et al. have reported that DOPE-containing liposome/pDNA complexes aggregate with red blood cells and this interaction is one of the major factors involved in the instability and limited gene expression of the complexes after intravenous administration of DOPE containing liposome complexes [24]. Our results also showed that Man/DOPE liposome/pDNA complexes aggregate with cationic liposomes (Fig. 8). Therefore, this interaction will need to be prevented for more efficient targeted gene delivery. Recently, Eliyahu et al. investigated the interaction of blood components with pDNA/cationic liposome complexes under conditions relevant to in vivo intravenous administration [25]. In their report, the selection of medium (i.e. plasma and serum) and/or modification of cationic liposomes with 1% polyethylene glycol lipids reduced the aggregation of cationic liposome/pDNA complexes in the presence of erythrocytes. Thus, the use of these approaches may enhance the cell-specificity of pDNA complexed with Man liposomes. Further studies are needed to investigate the interaction with blood components and/or the synthesis of polyethylene glycol-grafted glycosylated lipids for cell-selective gene delivery.

In conclusion, DOPE in Man liposomes contributes to efficient gene expression in the target site through enhancing distribution to the target site and intracellular sorting in the target cells. However, destabilization before internalizing target cells might be a rate-limiting step for efficient gene delivery in DOPE-containing Man liposomes. The observations in this study show that, for efficient targeted gene delivery with cationic liposomes, it is essential to formulate lipoplexes in the light of a better understanding of the effect of lipids on their function and biodistribution under in vivo conditions. This information will be very useful for designing pDNA/ligand-grafted cationic liposome complexes for cell-specific gene delivery under in vivo conditions.

Acknowledgement

This work was supported in part by Grant-in-Aids for Scientific Research from the Ministry of Education, Culture, Sports, Science, and Technology of Japan, and by Health and Labour Sciences Research Grants for Research on Advanced Medical Technology from the Ministry of Health, Labour and Welfare of Japan.

References

[1] T. Ohashi, S. Boggs, P. Robbins, A. Bahnson, K. Patrene, F. Wei, J. Wei, J. Li, L. Lucht, Y. Fei, S. Clark, M. Kimak, H. He, P. Mowery-Rushton, J.A. Barranger, Efficient transfer and sustained high expression of the human glucocerebrosidase gene in mice and their functional macrophages following transplantation of bone marrow transduced by a retroviral

vector, Proc. Natl. Acad. Sci. U. S. A. 89 (23) (1992) 11332–11336.
[2] D.B. Kohn, N. Sarver, Gene therapy for HIV-1 infection, Adv. Exp. Med. Biol. 394 (1996) 421–428.
[3] S.E. Raper, N. Chirmule, F.S. Lee, N.A. Wivel, A. Bagg, G. Gao, J.M. Wilson, M.L. Batshaw, Fatal systemic inflammatory response syndrome in an ornithine transcarbamylase deficient patient following adenoviral gene transfer, Mol. Genet. Metab. 80 (1–2) (2003) 148–158.
[4] R.I. Mahato, Y. Takakura, M. Hashida, Nonviral vectors for in vivo gene delivery: physicochemical and pharmacokinetic considerations, Crit. Rev. Ther. Drug Carr. Syst. 14 (2) (1997) 133–172.
[5] L. Huang, S. Li, Liposomal gene delivery: a complex package, Nat. Biotechnol. 15 (1997) 620–621.
[6] M. Hashida, M. Nishikawa, F. Yamashita, Y. Takakura, Cell-specific delivery of genes with glycosylated carriers, Adv. Drug Deliv. Rev. 52 (3) (2001) 187–196.
[7] P. Erbacher, M.T. Bousser, J. Raimond, M. Monsigny, P. Midoux, A.C. Roche, Gene transfer by DNA/glycosylated polylysine complexes into human blood monocyte-derived macrophages, Hum. Gene Ther. 7 (6) (1996) 721–729.
[8] S. Kawakami, A. Sato, M. Nishikawa, F. Yamashita, M. Hashida, Mannose receptor-mediated gene transfer into macrophages using novel mannosylated cationic liposomes, Gene Ther. 7 (4) (2000) 292–299.
[9] Y. Hattori, S. Kawakami, S. Suzuki, F. Yamashita, M. Hashida, Enhancement of immune responses by DNA vaccination through targeted gene delivery using mannosylated cationic liposome formulations following intravenous administration in mice, Biochem. Biophys. Res. Commun. 317 (4) (2004) 992–999.
[10] S. Kawakami, F. Yamashita, K. Nishida, J. Nakamura, M. Hashida, Glycosylated cationic liposomes for cell-selective gene delivery, Crit. Rev. Ther. Drug Carr. Syst. 19 (2) (2002) 171–190.
[11] S. Kawakami, A. Sato, M. Yamada, F. Yamashita, M. Hashida, The effect of lipid composition on receptor-mediated in vivo gene transfection using mannosylated cationic liposomes in mice, STP Pharma. Sci. 11 (1) (2001) 117–120.
[12] S. Kawakami, Y. Hattori, Y. Lu, Y. Higuchi, F. Yamashita, M. Hashida, Effect of cationic charge on receptor-mediated transfection using mannosylated cationic liposome/plasmid DNA complexes following the intravenous administration in mice, Pharmazie 59 (5) (2004) 405–408.
[13] M. Yamada, M. Nishikawa, S. Kawakami, Y. Hattori, T. Nakano, F. Yamashita, M. Hashida, Tissue and intrahepatic distribution and subcellular localization of a mannosylated lipoplex after intravenous administration in mice, J. Control. Release 98 (1) (2004) 157–167.
[14] J.H. Felgner, R. Kumar, C.N. Sridhar, C.J. Wheeler, Y.J. Tsai, R. Border, P. Ramsey, M. Martin, P.L. Felgner, Enhanced gene delivery and mechanism studies with a novel series of cationic lipid formulations, J. Biol. Chem. 269 (4) (1994) 2550–2561.
[15] D.C. Litzinger, L. Huang, Phosphatidylethanolamine liposomes: drug delivery, gene transfer and immunodiagnostic applications, Biochim. Biophys. Acta 1113 (2) (1992) 201–227.
[16] H. Farhood, N. Serbina, L. Huang, The role of dioleoyl phosphatidylethanolamine in cationic liposome mediated gene transfer, Biochim. Biophys. Acta 1235 (2) (1995) 289–295.
[17] J.Y. Legendre, F.C. Szoka, Delivery of plasmid DNA into mammalian cell lines using pH-sensitive liposomes: comparison with cationic liposomes, Pharm. Res. 9 (10) (1992) 1235–1242.
[18] F. Sakurai, T. Nishioka, H. Saito, T. Baba, A. Okuda, O. Matsumoto, T. Taga, F. Yamashita, Y. Takakura, M. Hashida, Interaction between DNA-cationic liposome complexes and erythrocytes is an important factor in systemic gene transfer via the intravenous route in mice: the role of the neutral helper lipid, Gene Ther. 8 (9) (2001) 677–686.
[19] Y. Liu, L.C. Mounkes, H.D. Liggitt, C.S. Brown, I. Solodin, T.D. Heath, R.J. Debs, Factors influencing the efficiency of cationic liposome-mediated intravenous gene delivery, Nat. Biotechnol. 15 (2) (1997) 167–173.
[20] S. Fumoto, S. Kawakami, M. Ishizuka, M. Nishikawa, F. Yamashita, M. Hashida, Analysis of hepatic disposition of native and galactosylated polyethylenimine complexed with plasmid DNA in perfused rat liver, Drug Metab. Pharmacokineti. 18 (4) (2003) 230–237.
[21] K. Ogawara, S. Hasegawa, M. Nishikawa, Y. Takakura, M. Hashida, Pharmacokinetic evaluation of mannosylated bovine serum albumin as a liver cell-specific carrier: quantitative comparison with other hepatotropic ligands, J. Drug Target. 6 (5) (1999) 349–360.
[22] M. Nishikawa, M. Yamauchi, K. Morimoto, E. Ishida, Y. Takakura, M. Hashida, Hepatocyte-targeted in vivo gene expression by intravenous injection of plasmid DNA complexed with synthetic multi-functional gene delivery system, Gene Ther. 7 (7) (2000) 548–555.
[23] P. Midoux, A. Kichler, V. Boutin, J.C. Maurizot, M. Monsigny, Membrane permeabilization and efficient gene transfer by a peptide containing several histidines, Bioconjug. Chem. 9 (2) (1998) 260–267.
[24] F. Sakurai, T. Nishioka, F. Yamashita, Y. Takakura, M. Hashida, Effects of erythrocytes and serum proteins on lung accumulation of lipoplexes containing cholesterol or DOPE as a helper lipid in the single-pass rat lung perfusion system, Eur. J. Pharm. Biopharm. 52 (2) (2001) 165–172.
[25] H. Eliyahu, N. Servel, A.J. Domb, Y. Barenholz, Lipoplex-induced hemagglutination: potential involvement in intravenous gene delivery, Gene Ther. 9 (13) (2002) 850–858.
[26] M. Nishikawa, Y. Ohtsubo, J. Ohno, T. Fujita, Y. Koyama, F. Yamashita, M. Hashida, H. Sezaki, Pharmacokinetics of receptor-mediated hepatic uptake of glycosylated albumin in mice, Int. J. Pharm. 85 (1–3) (1992) 75–85.
[27] T. Fujita, M. Nishikawa, C. Tamaki, Y. Takakura, M. Hashida, H. Sezaki, Targeted delivery of human recombinant superoxide dismutase by chemical modification with mono- and polysaccharide derivatives, J. Pharmacol. Exp. Ther. 263 (3) (1992) 971–978.

[28] Y.C. Lee, C.P. Stowell, M.J. Krantz, 2-Imino-2-methoxyethyl 1-thioglycosides: new reagents for attaching sugars to proteins, Biochemistry 15 (18) (1976) 3956–3963.
[29] S. Kawakami, F. Yamashita, M. Nishikawa, Y. Takakura, M. Hashida, Asialoglycoprotein receptor-mediated gene transfer using novel galactosylated cationic liposomes, Biochem. Biophys. Res. Commun. 252 (1) (1998) 78–83.
[30] G.R. Bartlett, Phosphorus assay in column chromatography, J. Biol. Chem. 234 (3) (1959) 466–468.
[31] C. Wang, R.L. Smith, Lowry determination of protein in the presence of Triton X-100, Anal. Biochem. 63 (2) (1975) 414–417.
[32] S. Fumoto, F. Nakadori, S. Kawakami, M. Nishikawa, F. Yamashita, M. Hashida, Analysis of hepatic disposition of galactosylated cationic liposome/plasmid DNA complexes in perfused rat liver, Pharm. Res. 20 (9) (2003) 1452–1459.
[33] S. Li, W.C. Tseng, D.B. Stolz, S.P. Wu, S.C. Watkins, L. Huang, Dynamic changes in the characteristics of cationic lipidic vectors after exposure to mouse serum: implications for intravenous lipofection, Gene Ther. 6 (4) (1999) 585–594.

Available online at www.sciencedirect.com
SCIENCE DIRECT®
Journal of Controlled Release 107 (2005) 373–382
journal of controlled release
www.elsevier.com/locate/jconrel
GENE DELIVERY

Intracellular distribution of NFκB decoy and its inhibitory effect on TNFα production by LPS stimulated RAW 264.7 cells

Yuriko Higuchi [a], Shigeru Kawakami [a], Makiya Nishikawa [b], Fumiyoshi Yamashita [a], Mitsuru Hashida [a,*]

[a] *Department of Drug Delivery Research, Graduate School of Pharmaceutical Sciences, Kyoto University, Sakyo-ku, Kyoto 606-8501, Japan*
[b] *Department of Biopharmaceutics and Drug Metabolism, Graduate School of Pharmaceutical Sciences, Kyoto University, Sakyo-ku, Kyoto 606-8501, Japan*

Received 13 December 2004; accepted 6 July 2005
Available online 24 August 2005

Abstract

Nuclear factor kappa B (NFκB) is a transcriptional factor for the expression of many cytokines that are involved in the pathogenesis of inflammatory diseases. Unstimulated NFκB sequestered in the cytoplasm bound to inhibitory proteins is called IκBs. Many activators of NFκB cause degradation of IκB proteins and free NFκB can enter the nucleus and induce gene expression. In this study, we analyzed the relationship between the intracellular distribution and pharmacological effect of NFκB decoy in RAW 264.7 cells. Most of the fluorescent labeled NFκB decoy was observed in the cytoplasm both with or without cationic transfection without LPS stimulation. Furthermore, under LPS stimulation, most of NFκB decoy was also observed in the cytoplasm. However, NFκB decoy effectively inhibited the production of TNFα in RAW 264.7 cells. The inhibitory effect of TNFα production by NFκB decoy transfected by cationic liposomes was much stronger than that by naked NFκB decoy, because the amount of cellular association of NFκB transfected by cationic liposome decoy was 7 times higher than that of naked NFκB decoy. This information is of great value for the design of NFκB decoy carrier systems.

Keywords: NFκB; NFκB decoy; Cellular distribution; TNFα; Cationic liposome

1. Introduction

Nuclear factor kappa B (NFκB) is a transcriptional factor, which can be activated by a variety of stimuli such as bacterial endotoxins, ionizing radiation, oxidative stress and certain chemical agents [1]. NFκB is a central regulator of the inflammatory response and is critical for the transcription of multiple proinflammatory molecules, including TNFα, IL-1, IL-2, IL-6, IL-8, IL-12, and IFN-β, etc. [1,2]. Therefore, NFκB decoy, which attenuates NFκB-mediated gene expression, has been applied to glomerulonephritis [3], hyperplasia after angioplasty [4], atopic dermatitis [5], ischemia/reperfusion [6], and endotoxin-induced liver injury [7] etc. However, these in vivo applications

* Corresponding author. Fax: +81 75 753 4575.
E-mail address: hashidam@pharm.kyoto-u.ac.jp (M. Hashida).

0168-3659/$ - see front matter © 2005 Elsevier B.V. All rights reserved.
doi:10.1016/j.jconrel.2005.07.004

are carried out by local administration of naked NFκB decoy or that incorporated in HVJ liposomes, fusogenic liposomes, because of the problem about the stability or lack of cell-specificity.

For the wider clinical application involving NFκB decoy therapy, it is necessary to develop a non-invasive form of gene delivery, which should be safe for repetitive use and provide reproducible therapeutic effects. To achieve this goal, a thorough understanding of the intracellular disposition characteristics of NFκB decoy, and its carrier systems is important for assessing the availability of administered gene drugs because there is at present little information on the pharmacokinetics of NFκB decoy including its target site.

It has been reported that NFκB in unstimulated cells is sequestered in the cytoplasm through interaction with a class of inhibitory proteins called IκBs (IκB-α, -β, and -ε) [8–13] but stimuli such as lipopolysaccharide (LPS) enhance the degradation of IκB proteins; consequently, free NFκB can enter the nucleus and induce gene expression [14]. Therefore, the intracellular fate of NFκB decoy with or without stimuli may be different although this is not yet clear. In this study, RAW 264.7 cells, a macrophage cell line, was selected for the evaluation of NFκB decoy characteristics, because most cytokines are produced by macrophages.

The purpose of this study was to analyze the relationship between the intracellular distribution and pharmacological effect of NFκB decoy. In the present study, we examined the intracellular distribution of fluorescence-NFκB decoy in RAW 264.7 cells with or without LPS by confocal microscopy study and investigated the TNFα production (pharmacological effect). It was demonstrated that NFκB decoy remaining in the cytoplasm is effectively bound to NFκB and inhibits TNFα produced in macrophages and cationic liposomes that could enhance the pharmacological effects of NFκB decoy in macrophages. This information is of great value for design of NFκB decoy carrier systems.

2. Materials and methods

2.1. Chemicals

NFκB decoy and control oligonucleotides used in this study are phosphorothioate double stranded oligonucleotides. Their sequences are as follows: 20mer NFκB decoy 5′-CCTTGAAGGGATTTCCC-TCC-3′ (A)/ 3′-GGAACTTCCCTAAAGGGAGG-5′ (B), control oligonucleotides 5′-CATGTCGTCACTG-CGCTCAT-3′/3′-GTACAGCAGTGACGCGAGTA-5′. These oligonucleotides were kindly provided by Anges MG Inc. (Osaka, Japan). Lipopolysaccharide (LPS) from Salmonella Minnesota Re 595 (Re mutant), L-glutamine, penicillin, and streptomycin were purchased from Sigma Chemicals Inc. (St. Louis, MO, USA). RPMI 1640 medium was obtained from Nissui Pharmaceutical Co. (Tokyo, Japan). [$\gamma-^{32}$P] ATP was purchased from Amersham Biosciences Co. (Piscataway, NJ, USA). Opti-MEM® I and fetal bovine serum (FBS) and Oligofectamine® were obtained from Invitrogen Co. (Carlsbad, CA, USA). OptEIA™ were purchased from BD Biosciences Pharmingen, (San Diego, CA, USA). Enzyme Immunoassay for NFκB Product No. TF 01 was purchased from Oxford biomedical research, Inc. (Oxford, MI, USA). All other chemicals were of the highest purity available.

2.2. Cell culture

RAW 264.7 cells, a murine macrophage-like cell line, were cultured with RPMI 1640 medium supplemented with 10% FBS, 2 mM L-glutamine, 100 U/ml penicillin G, and 0.1 mg/ml streptomycin. Cells were maintained at 37 °C with 5% CO_2 in a humidified incubator. Cells were plated on a 12-well culture plate for the confocal microscopy study at a density of 1.3×10^5 cells/cm^2 and cultured for 24 h. In addition, cells were plated on a 24-well culture plate for the TNF-α secretion study and the uptake experiment at a density of 1.3×10^5 cells/cm^2.

2.3. Confocal laser scanning microscopy study

RAW 264.7 cells cultured on micro cover glasses (Matsumani, glass IND, LTD., Osaka, Japan) were washed 3-times with 1 ml cold PBS, and incubated with 1 ml FITC-labeled decoy oligonucleotide in Opti-MEM® (2 μM) for the indicated time with or without 4 h LPS treatment. Cells were washed 3 times with cold PBS and fixed with 4% paraformaldehyde for 15 min. For nuclei staining, fixed cells were permiabilized with 0.2% Triton X-100-PBS for

20 min. Cell nuclei were stained by incubation with 0.5 μg/ml propidium iodide (PI) in 0.1 M NaCl–0.1 M Tris–HCl (pH 7.4) at room temperature for 20 min, following treatment with 15 μg/ml Rnase A (Roche Diagnostics Co., Indianapolis, IN, USA). After cells were washed once with 1 ml cold phosphate buffered saline (PBS), cover glasses were mounted on slide glasses with 50% glycerol–2.5% DABCO (1,4-diazabicyclo-[2,2,2]octane) (Sigma Chemical Co., Inc., St. Louis, MO)-PBS. Then, cells were scanned using a confocal laser microscope (MRC-1024, Bio-Rad Laboratories, Inc., Hercules, CA, USA).

2.4. Cytokine secretion

RAW 264.7 cells were washed with PBS and incubated with or without naked decoy oligonucleotide in Opti-MEM® containing 0.01 μg/ml LPS for 4 h (Fig. 2). Oligofectamine® transfection was performed according to the manufacturer's instructions. After oligofectamine transfection, cells were washed with PBS followed by the addition of Opti-MEM® containing 0.01 μg/ml LPS and allowed to stand for 4 h (Fig. 7). Supernatants were collected for ELISA and kept at −80 °C. The levels of TNFα in the supernatants were determined by the OptEIA™ (BD Biosciences Pharmingen, San Diego, CA, USA).

2.5. Enzyme immunoassay (EIA)

The amount of NFκB in nuclear extracts of RAW 264.7 cells was evaluated by means of EIA for NFκB (Oxford biomedical research, Inc., Oxford, MI, USA). Nuclear extracts were prepared from RAW 264.7 cells, which were incubated with or without naked decoy oligonucleotide for 4 h in Opti-MEM® containing 0.01 μg/ml LPS, using of Nuclear/Cytosol Fraction Kit (Bio Vision Products, Mountain View, CA, USA).

2.6. Radiophosphorylation of oligonucleotides

Oligonucleotides were labeled with [γ−^{32}P] ATP using MEGALABEL™ 5′-End Labeling Kit (Takara Bio. Inc., Shiga, Japan). Briefly, 3 μl oligonucleotides (1.7 μM), 5 μl [γ−^{32}P] ATP (370 MBq/ml) and 1 μl T4 polynucleotide kinase were mixed in phosphorylation buffer. After 30 min incubation at 37 °C, the mixture was incubated for 10 min at 70 °C in order to inactivate T4 polynucleotide kinase. Then, the mixture was purified by gel chromatography using a NAP 10 column (Amersham Biosciences Co., Piscataway, NJ, USA) and eluted with 10 mM Tris–Cl and 1 mM EDTA (pH 8.0). The fractions containing the derivatives were selected based on their radioactivity.

2.7. Uptake experiment

After washing RAW 264.7 cells with 1 ml cold PBS, decoy oligonucleotides were added to the cells at a concentration of 0.1 μM 5′-[^{32}P]-labeled decoy nucleotide at about 100,000 cpm. At predetermined times, the supernatant was removed then cells were dissolved in 700 μl SOLUENE®-350 (Perkin Elmer Life and Analytical Sciences, Inc., Boston, MA, USA) and the radioactivity measured in a scintillation counter (LSA-500, Beckman, Tokyo, Japan) after neutralization with 1 M HCl and addition of 5 ml Clear-Sol I (Nacalai Tesque, Inc., Kyoto, Japan). To revise in cell number by the protein content, cells were washed 5-times with cold PBS and solubilized in 0.5 ml of Triton X-100 (0.1%) with 0.3 M NaOH. Aliquots were taken for determination of the protein content by Lowry methods.

2.8. Quantitative analysis of intracellular distribution of decoy

After washing RAW 264.7 cells with 1 ml cold PBS, Cells were incubated with 2 μM [^{32}P] naked NFκB decoy for 4 h in Opti-MEM® with or without LPS (0.01 μg/ml). or 0.2 μM [^{32}P] NFκB decoy complexed with cationic liposomes for 4 h in Opti-MEM® containing LPS (0.01 μg/ml). Oligofectamine® transfection was performed according to the manufacturer's instructions. After 0.2 μM [^{32}P] NFκB decoy complexed with oligofectamine was transfected, cells were incubated for 4 h in Opti-MEM® containing 0.01 μg/ml LPS. At 4 h, the supernatant was removed then cells were washed with cold PBS for five times. After cells were gently removed with cellscraper in 1 ml of cold PBS, cell suspension was separated to nuclear extracts and cytoplasmic extracts by Nuclear/Cytosol Fraction Kit (Bio Vision Products, Mountain View, CA,

USA). Both nuclear extracts and cytplasmic extracts were dissolved in 700 μl SOLUENE®-350 (Perkin Elmer Life and Analytical Sciences, Inc., Boston, MA, USA) and the radioactivity measured in a scintillation counter (LSA-500, Beckman, Tokyo, Japan) after neutralization with 1 M HCl and addition of 5 ml Clear-Sol I (Nacalai Tesque, Inc., Kyoto, Japan). To revise in cell number by the protein content, cells were washed 5-times with cold PBS and solubilized in 0.5 ml of Triton X-100 (0.1%) with 0.3 M NaOH. Aliquots were taken for determination of the protein content by Lowry methods.

2.9. Statistical analysis

Statistical comparisons were performed using Student's t test for two groups and a one-way ANOVA for multiple groups. A value of $P<0.05$ was considered to be indicative of statistical significance.

3. Results

3.1. Comparison of intracellular distribution of NFκB decoy with or without LPS treatment

It is well known that NFκB activated by LPS enters the nucleus and induces gene expression. The intracellular distribution of FITC-NFκB decoy was compared with and without LPS treatment (Fig. 1). No difference was found in these intracellular distribution patterns. In both images, most of FITC-NFκB decoys were observed in the cytoplasm. Moreover, in the case of single stranded oligonucleotides, the same as NFκB decoy (double

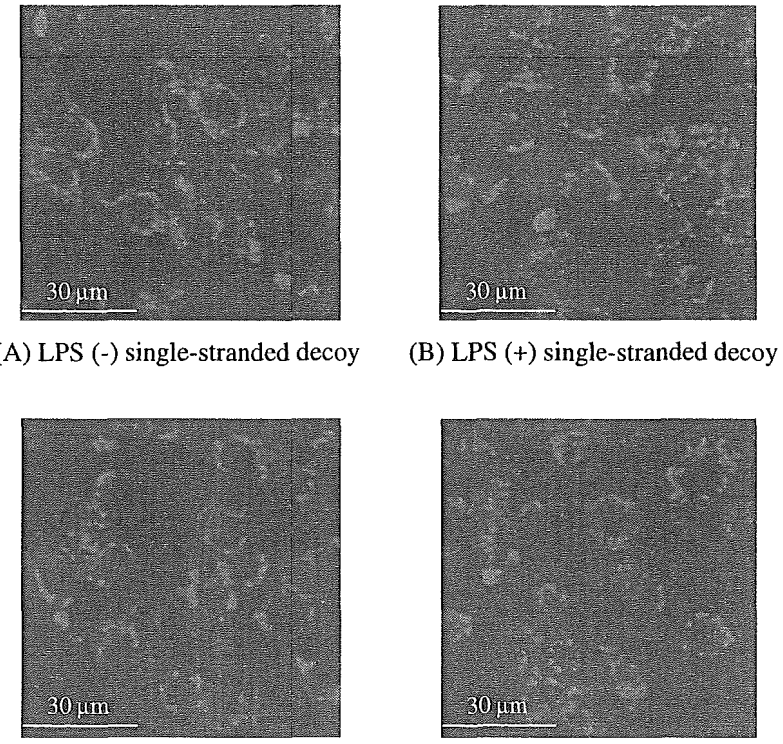

(A) LPS (-) single-stranded decoy (B) LPS (+) single-stranded decoy

(C) LPS (-) double-stranded decoy (D) LPS (+) double-stranded decoy

Fig. 1. The confocal microscopy images of FITC-decoy and single-stranded oligonucleotides in RAW 264.7 cells. Cells were incubated with 2 μM FITC-decoy and single-stranded oligonucleotides in Opti-MEM® at 37 °C for 4 h. Cells were washed with PBS and fixed with 4% paraformaldehyde.

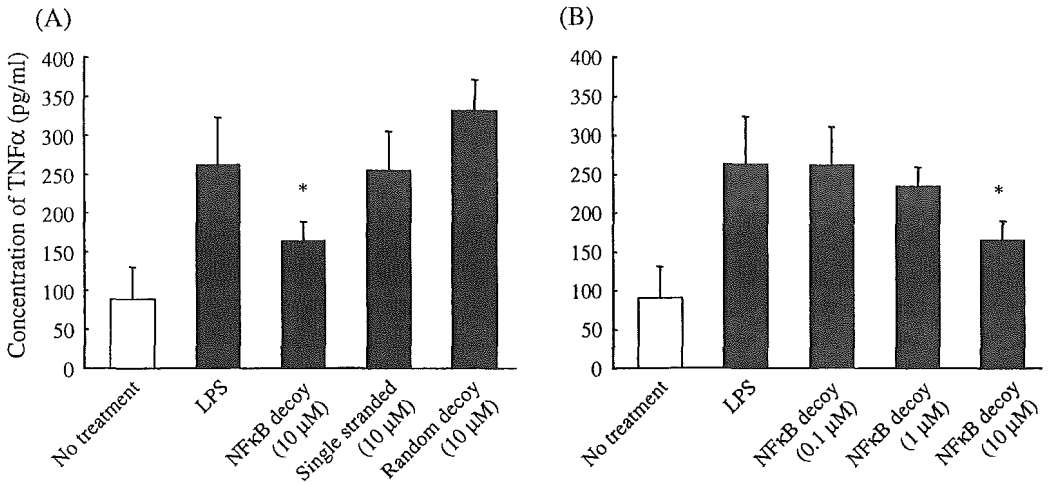

Fig. 2. Inhibition of TNFα secretion of RAW 264.7 cells treated with LPS by naked decoy and single-stranded oligonucleotides. (A) Cells were incubated with or without 10 μM decoy (NFκB decoy or scramble decoy) and single-stranded oligonucleotides for 4 h in Opti-MEM® containing LPS (0.01 μg/ml). (B) Cells were incubated with or without decoy NFκB decoy (0.1, 1 and 10 μM) for 4 h in Opti-MEM® containing LPS (0.01 μg/ml). Supernatant was collected and its TNFα concentration measured by ELISA. Each result represents the mean ± S.D. ($n=3$). Statistically significant differences ($^*P<0.05$) from LPS only or random decoy.

stranded oligonucleotides), there was no difference in the intracellular distribution of single oligonucleotides with and without LPS treatment.

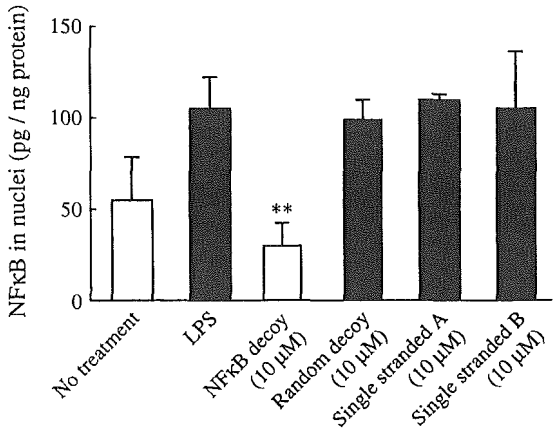

Fig. 3. EIA for activated NFκB in nuclear extract of RAW 264.7 cells. Cells were incubated with or without naked decoy (NFκB decoy or scramble decoy) and single-stranded oligonucleotides (10 μM) for 4 h in Opti-MEM® containing LPS (0.01 μg/ml). After washing with PBS, the cells were collected and nuclear proteins were extracted.

3.2. Inhibitory effect of TNFα secretion by naked NFκB decoy

TNFα secretion was significantly inhibited by the presence of 10 μM naked NFκB decoy (Fig.

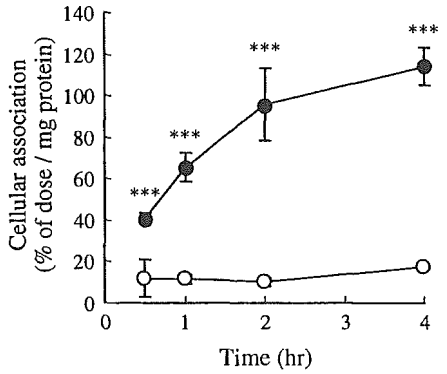

Fig. 4. The cellular association of [^{32}P]-labeled NFκB decoy with (●) or without (○) cationic liposome transfection in RAW 264.7 cells. Cells were incubated with 0.2 μM [^{32}P]-labeled NFκB decoy with or without cationic liposome at 37 °C in Opti-MEM® for 0.5, 1, 2 and 4 h. Each result represents the mean ± S.D. ($n=3$). Statistically significant differences ($^{***}P<0.001$) from naked NFκB decoy.

2A). At the concentration of 0.1 and 1 μM naked NFκB decoy, the inhibition was not observed (Fig. 2B).

Single stranded NFκB decoy and random decoy could not inhibit TNFα secretion, suggesting the double stranded NFκB decoy efficiently inhibited the NFκB mediated transcription.

3.3. Inhibitory effect of NFκB translocation in the nucleus by naked NFκB decoy

The amount of NFκB in the nucleus was determined by EIA (Fig. 3). Following LPS treatment, the amount of NFκB in the nucleus significantly increased, while the amount of NFκB in the nuclei did not increase by the addition of NFκB decoy inhibited the increase of NFκB in the nucleus. On the other hand, scramble decoy and single stranded oligonucleotides (both sequence A and B) did not inhibit the increase of NFκB in the nucleus.

3.4. Quantitative analysis of the cellular association of 5′-[^{32}P]-labeled decoy with or without cationic liposomes

The amount of cellular association of 5′-[^{32}P]-labeled decoy with or without cationic liposomes is compared in Fig. 4. Time-dependant uptake was observed both in the uptake of naked decoy and cationic liposome-transfected decoy. The amount of cellular association of decoy with cationic transfection was much higher than that of naked decoy. At the medium collection time point of the TNFα secretion experiment (4 h), the cellular association of decoy with cationic transfection was approximately 7-times higher than for naked decoy.

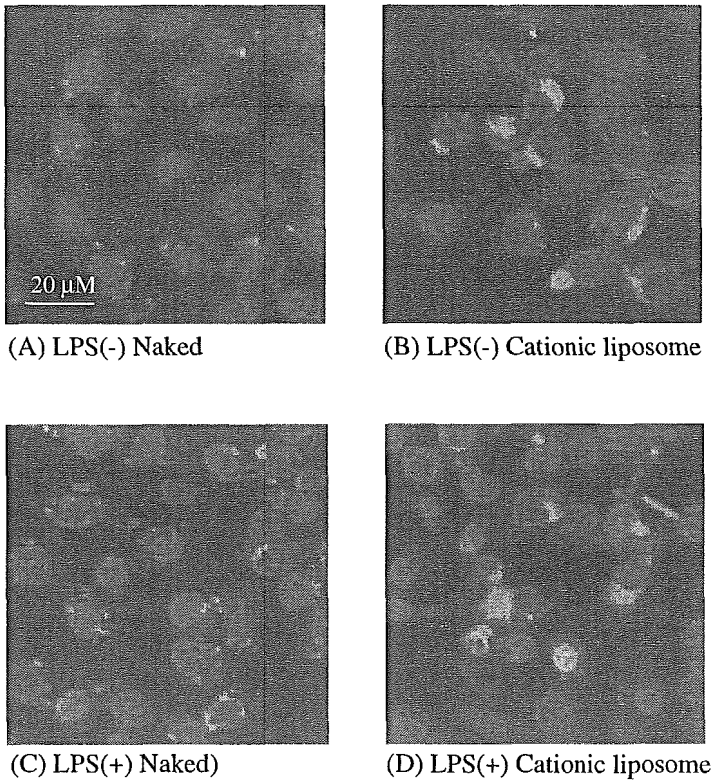

(A) LPS(-) Naked (B) LPS(-) Cationic liposome

(C) LPS(+) Naked) (D) LPS(+) Cationic liposome

Fig. 5. Intracellular distribution of naked FITC-NFκB decoy (green) (A), (C) or FITC-NFκB decoy (green) complexed with cationic liposome (B), (D) in RAW 264.7 cells. Cells were incubated with naked FITC-NFκB decoy (2 μM) for 4 h without (A) or with (C) LPS (0.01 μg/ml). Cells were incubated with FITC-NFκB decoy (0.2 μM) complexed with cationic liposome for 4 h without (B) or with (D) LPS (0.01 μg/ml). After cells were washed with PBS and fixed with 4% paraformaldehyde, nuclei were stained by propidium iodide (red). (For interpretation of the references to colour in this figure legend, the reader is referred to the web version of this article.)

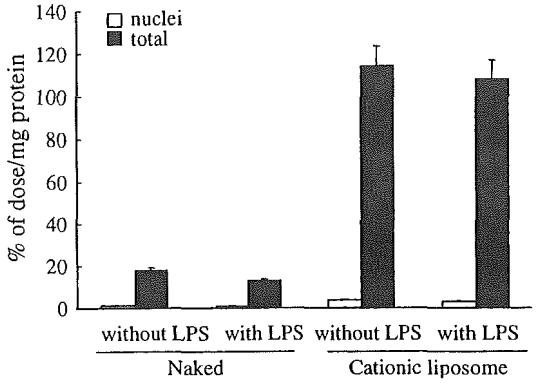

Fig. 6. The quantitative analysis for intracellular distribution of [^{32}P] NFκB decoy in RAW 264.7 cells. Cells were incubated with 2 μM [^{32}P] naked NFκB decoy or 0.2 μM [^{32}P] NFκB decoy complexed with cationic liposomes for 4 h in Opti-MEM® containing LPS (0.01 μg/ml). After cells were washed with PBS, radioactivity of whole cell or nuclear extract was measured. Statistically significant differences (**$P<0.01$) from only LPS stimulation.

3.5. Effect of LPS and cationic liposomes on the intracellular distribution of FITC-NFκB

In the case of naked NFκB decoy, there was no difference in the distribution of FITC-NFκB decoy without (Fig. 5 (A)) and with (Fig. 5 (C)) LPS. Most of FITC-NFκB was observed in cytoplasm. On the other hand, in the case of transfection of FITC-NFκB decoy complexed with cationic liposomes, a little more FITC-NFκB decoy was observed in nuclei comparing to naked FITC-NFκB decoy. However, most of complex was observed in cytoplasm both without (Fig. 5 (B)) and with (Fig. 5 (D)).

3.6. Quantitative analysis of intracellular distribution of 5′-[^{32}P]-labeled NFκB decoy

For more quantitative analysis, intracellular distribution of 5′-[^{32}P]-labeled NFκB decoy was compared with and without LPS treatment (Fig. 6). In the case of naked NFκB decoy, the accumulation in nuclei was about 10% of total cellular accumulation. In the case of NFκB decoy complexed with cationic liposomes, total cellular uptake was about 7 times higher than naked NFκB decoy. Although nuclear accumulation of NFκB decoy was also higher than naked NFκB decoy, the accumulation in nuclei was about 7% of total cellular accumulation. LPS did not affect the nuclear/total accumulation ratio.

3.7. Inhibition effect of TNFα secretion by naked NFκB transfected with cationic liposomes

TNFα secretion was significantly inhibited by the presence of 0.2 μM NFκB decoy transfected with cationic liposomes (Fig. 7) compared with the control cell treated with LPS and empty cationic liposomes. However, single stranded NFκB decoy and random decoy could not inhibit TNFα secretion. This observation is well corresponding to the result of naked decoy and single stranded oligonucleotide (Fig. 1A). In the case of naked NFκB decoy, inhibitory effect was not observed even at 1 μM naked NFκB decoy, however 10 μM naked NFκB decoy well inhibited the TNFα secretion (Fig. 1B). On the contrary, 50-times lower concentration of NFκB decoy (0.2 μM) transfected with cationic liposomes achieved the same degree of inhibitory effect of TNFα secretion (Fig. 7).

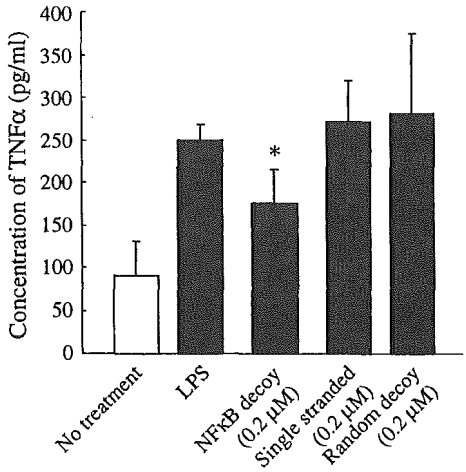

Fig. 7. TNFα secretion of RAW 264.7 cells treated with LPS (0.01 μg/ml) was inhibited by decoy and single stranded oligonucleotides (0.2 μM) transfected with cationic liposomes. Cells were incubated with decoy (NFκB decoy or scramble decoy) and single-stranded oligonucleotides for 4 h in Opti MEM containing LPS. Supernatant was collected and TNFα concentration was measured by ELISA. Each result represents the mean ± S.D. ($n=3$). Statistically significant differences (*$P<0.05$) from LPS only, single-stranded oligonucleotide or random decoy.

4. Discussion

In this study, we investigated the relationship between the intracellular distribution and pharmacological effect of NFκB decoy. Focusing on the intracellular distribution of NFκB decoy, we and another group have reported that confocal microscopy is the most suitable and convenient method of investigation [15]. Therefore, the fluorescent NFκB decoy distribution was evaluated by confocal microscopy.

Without LPS stimulation, it is well known that NFκB/IκB complex is still formed in the cell [14]; therefore, the inherent intracellular distribution of NFκB decoy can be analyzed. Generally, NFκB decoy is expected to enter the nuclei, because the size of the NFκB decoy used in this study is small (13 kDa) enough to distribute in the nuclei [16]. However, the confocal microscopic images showed that most of NFκB decoy was present only in the cytoplasm of cells without LPS treatment (Fig. 1), suggesting that NFκB decoy without binding NFκB is not distributed in the nuclei in spite of its small size.

Then, the intracellular distribution of NFκB decoy was studied by LPS stimulation. After LPS stimulation, IκB in NFκB/IκB complex is degraded and, consequently, NFκB decoy could bind to NFκB. The nuclear localization sequence of NFκB is not masked by NFκB decoy [17,18]; thus, NFκB decoy is expected to distribute to the nuclei under the influence of NFκB. Surprisingly, it was found that most of NFκB decoy (Fig. 1B, D) was only entrapped in the cytoplasm in LPS stimulated cells. In the case of cationic liposome transfection of NFκB decoy, although a little of NFκB decoy was observed in the nucleus, most of them observed in the cytoplasm (Fig. 5B, D). This in vitro result observed by RAW 264.7 cells agrees with the in vitro distribution results reported by Griesenbach et al. [19] showing that most of NFκB decoy complexed with liposomes was located in the cytoplasm of a cystic fibrosis airway epithelial cell line. For a more quantitative analysis of intracellular distribution, the accumulation of [^{32}P] labeled NFκB decoy was evaluated by measuring the radioactivity in the nucleus or in the cells (Fig. 6). The accumulation of [^{32}P] labeled decoy in the nuclei was about 10% of total cellular accumulation. This in vitro result agrees with confocal microscopic study. In previous study, we showed that the intracellular distribution of antisense DNA (single stranded) was different to the kind of cell. Transfected antisense DNA with cationic liposome easily moved to the nucleolus in U937 (human promonocytic leukemia) [21] cells but not in macrophages [22]. Our result in this study was agreed with them.

Previous study revealed that NFκB decoy could alternate the gene expression [23–25]. In this study, we focused the pharmacological effect NFκB decoy on macrophages and investigated the inhibitory effect of NFκB decoy on the production of TNFα. Inhibition of TNFα by NFκB decoy complexed with cationic liposomes was much higher than that of naked NFκB decoy (Figs. 2, 7). Therefore, NFκB decoy complexed with cationic liposomes was selected for discussing the relationship between the intracellular distribution and pharmacological effect of NFκB decoy in LPS stimulated cells. The confocal microscopy image (Fig. 1), TNFα inhibition study (Fig. 2) suggested that the action site of NFκB decoy is the cytoplasm. Furthermore, to reveal that this pharmacological effect is based on the inhibition effect of NFκB activation, NFκB content in the nuclei was determined by EIA (Fig. 3). The increase of NFκB in the nuclei was significantly inhibited by the addition of NFκB decoy complex. These results could be of great interest to determine the effects of NFκB decoy on transcription of TNFα. And the result of intracellular distribution and therapeutic effect of NFκB decoy complexed with cationic liposome was well compatible with the results of Griesenbach et al. [19]. However, this finding is inconsistent with the results of Griesenbach et al. that showed that cytoplasmic NFκB decoy has little pharmacological effect on bleomycin-induced pulmonary inflammation in vivo [20]. However, in vivo studies involve various complicating factors including the stability of NFκB decoy, interaction with endogenous components, and uptake by non-target cells: so their conclusion may involve other factors.

For a more quantitative analysis, the accumulation of [^{32}P] labeled NFκB decoy was evaluated by measuring the radioactivity in the cells. In this experiment, we can analyze the cellular association and amount of uptake of NFκB decoy with or without cationic liposomes. The cellular accumulation of [^{32}P] labeled NFκB decoy complex with cationic liposomes was 7 times higher than that of [^{32}P] labeled naked NFκB

decoy. This result is supported by the fact that NFκB decoy complexed with cationic liposomes more effectively inhibited TNFα production (Figs. 2B, 7). As far as the uptake mechanism is concerned, we have demonstrated that uptake of NFκB decoy under normal conditions without LPS stimulation was also energy-dependent. The uptake of [^{32}P] labeled decoy and single stranded oligonucleotides was significantly lower at 4 °C than at 37 °C (Data not shown). To date, it has been reported that antisense DNA, a single-stranded oligonucleotide is taken up by scavenger-like receptor-mediated endocytosis [26,27], adsorptive endocytosis and/or fluid-phase pinocytosis [28,29]. Taking this into consideration, NFκB decoy used in this study might be also taken up by a similar mechanism with single-stranded oligonucleotide. Although further experiment will be need, these results would provide the basic information to design the NFκB carrier.

In this study, we have demonstrated that naked NFκB decoy is not effective in a macrophage cell line because of the low uptake, however, cationic liposomes enhance the pharmacological effects of NFκB decoy. This result agrees with the fact that there have been very few preclinical trials using naked NFκB decoy and several vectors have been used in current preclinical approaches, such as HVJ liposomes [3,4,7], and cationic liposomes [6] directly administered the disease site [5]. To establish decoy therapy in a non-invasive manner, direct injection is not practical. However, the use of HVJ liposomes fails to achieve cell-specific gene delivery because its transfection mechanism involves non-specific membrane fusion. As far as cationic liposomes are concerned, a number of receptor-mediated gene delivery systems based on cationic liposomes have been developed to introduce foreign DNA into specific cell types in vivo [30]. It is well known that the target cells of NFκB decoy are macrophages; therefore macrophage-selective gene targeting by intravenous injection is of great importance. Previously, we reported successful pDNA delivery by intravenous administration targeting macrophages using mannosylated cationic liposomes, recognized by novel mannose receptors especially expressed on macrophages [31–34]. Therefore, our mannosylated cationic liposomes might be successful in systemically NFκB decoy therapy following intravenous administration in the future.

In conclusion, we have demonstrated that NFκB decoy is only located in the cytoplasm and that it inhibits TNFα production in RAW 264.7 cells. Also, cationic liposomes enhance the pharmacological effect of NFκB decoy by increasing its uptake. This information is of value for the carrier design of NFκB decoys that will enable non-invasive therapy to be carried out.

Acknowledgements

This work was supported in part by Grant-in-Aids for Scientific Research from Ministry of Education, Culture, Sports, Science, and Technology of Japan, and by Health and Labor Sciences Research Grants for Research on Hepatitis and BSE from the Ministry of Health, Labor and Welfare of Japan and by 21st Century COE Program "Knowledge Information Infrastructure for Genome Science".

References

[1] H.L. Pahl, Activators and target genes of Rel/NF-kappaB transcription factors, Oncogene 18 (1999) 6853–6866.
[2] T.S. Blackwell, J.W. Christman, The role of nuclear factor-kappa B in cytokine gene regulation, Am. J. Respir. Cell Mol. Biol. 17 (1997) 3–9.
[3] N. Tomita, R. Morishita, H.Y. Lan, K. Yamamoto, M. Hashizume, M. Notake, K. Toyosawa, B. Fujitani, W. Mu, D.J. Nikolic-Paterson, R.C. Atkins, Y. Kaneda, J. Higaki, T. Ogihara, In vivo administration of a nuclear transcription factor-kappaB decoy suppresses experimental crescentic glomerulonephritis, J. Am. Soc. Nephrol. 11 (2000) 1244–1252.
[4] S. Yoshimura, R. Morishita, K. Hayashi, K. Yamamoto, H. Nakagami, Y. Kaneda, N. Sakai, T. Ogihara, Inhibition of intimal hyperplasia after balloon injury in rat carotid artery model using *cis*-element 'decoy' of nuclear factor-kappaB binding site as a novel molecular strategy, Gene Ther. 8 (2001) 1635–1642.
[5] H. Nakamura, M. Aoki, K. Tamai, M. Oishi, T. Ogihara, Y. Kaneda, R. Morishita, Prevention and regression of atopic dermatitis by ointment containing NF-kB decoy oligodeoxynucleotides in NC/Nga atopic mouse model, Gene Ther. 9 (2002) 1221–1229.
[6] C. Kupatt, R. Wichels, M. Deiss, A. Molnar, C. Lebherz, P. Raake, G. von Degenfeld, D. Hahnel, P. Boekstegers, Retroinfusion of NFkappaB decoy oligonucleotide extends cardioprotection achieved by CD18 inhibition in a preclinical study of myocardial ischemia and retroinfusion in pigs, Gene Ther. 9 (2002) 518–526.
[7] I. Ogushi, Y. Iimuro, E. Seki, G. Son, T. Hirano, T. Hada, H. Tsutsui, K. Nakanishi, R. Morishita, Y. Kaneda, J. Fujimoto,

Nuclear factor kappa B decoy oligodeoxynucleotides prevent endotoxin-induced fatal liver failure in a murine model, Hepatology 38 (2003) 335–344.

[8] T. Hanada, A. Yoshimura, Regulation of cytokine signaling and inflammation, Cytokine Growth Factor Rev. 13 (2002) 413–421.

[9] S. Malek, Y. Chen, T. Huxford, G. Ghosh, IkappaBbeta, but not IkappaBalpha, functions as a classical cytoplasmic inhibitor of NF-kappaB dimers by masking both NF-kappaB nuclear localization sequences in resting cells, J. Biol. Chem. 276 (2001) 45225–45235.

[10] S.T. Whiteside, J.C. Epinat, N.R. Rice, A. Israel, I kappa B epsilon, a novel member of the I kappa B family, controls RelA and cRel NF-kappa B activity, EMBO J. 16 (1997) 1413–1426.

[11] P.A. Baeuerle, D. Baltimore, I kappa B: a specific inhibitor of the NF-kappa B transcription factor, Science 242 (1988) 540–546.

[12] J.E. Thompson, R.J. Phillips, H. Erdjument-Bromage, P. Tempst, S. Ghosh, I kappa B-beta regulates the persistent response in a biphasic activation of NF-kappa B, Cell 80 (1995) 573–582.

[13] S. Simeonidis, S. Liang, G. Chen, D. Thanos, Cloning and functional characterization of mouse IkappaBepsilon, Proc. Natl. Acad. Sci. U. S. A. 94 (1997) 14372–14377.

[14] S. Ghosh, M.J. May, E.B. Kopp, NF-kappa B and Rel proteins: evolutionarily conserved mediators of immune responses, Annu. Rev. Immunol. 16 (1998) 225–260.

[15] T. Takagi, M. Hashiguchi, R.I. Mahato, H. Tokuda, Y. Takakura, M. Hashida, Involvement of specific mechanism in plasmid DNA uptake by mouse peritoneal macrophages, Biochem. Biophys. Res. Commun. 245 (1998) 729–733.

[16] C.M. Feldherr, E. Kallenbach, N. Schultz, Movement of a karyophilic protein through the nuclear pores of oocytes, J. Cell Biol. 99 (1984) 2216–2222.

[17] F.E. Chen, D.B. Huang, Y.Q. Chen, G. Ghosh, Crystal structure of p50/p65 heterodimer of transcription factor NF-kappaB bound to DNA, Nature 391 (1998) 410–413.

[18] C.B. Phelps, L.L. Sengchanthalangsy, S. Malek, G. Ghosh, Mechanism of kappa B DNA binding by Rel/NF-kappa B dimers, J. Biol. Chem. 275 (2000) 24392–24399.

[19] U. Griesenbach, P. Scheid, E. Hillery, R. de Martin, L. Huang, D.M. Geddes, E.W. Alton, Anti-inflammatory gene therapy directed at the airway epithelium, Gene Ther. 7 (2000) 306–313.

[20] U. Griesenbach, R.L. Cassady, R.J. Cain, R.M. duBois, D.M. Geddes, E.W. Alton, Cytoplasmic deposition of NFkappaB decoy oligonucleotides is insufficient to inhibit bleomycin-induced pulmonary inflammation, Gene Ther. 9 (2002) 1109–1115.

[21] T. Kanamaru, T. Takagi, Y. Takakura, M. Hashida, Biological effects and cellular uptake of c-*myc* antisense oligonucleotides and their cationic liposome complex, J. Drug Target. 5 (1998) 235–246.

[22] T. Takagi, M. Hashiguchi, T. Hiramatsu, F. Yamashita, Y. Takakura, M. Hashida, Effect of cationic liposomes on intracellular trafficking and efficacy of antisense oligonucleotides in mouse peritoneal macrophages, J. Drug Target. 7 (2000) 363–371.

[23] A.K. Roshak, J.R. Jackson, K. McGough, M. Chabot-Fletcher, E. Mochan, L.A. Marshall, Manipulation of distinct NFκB proteins alters Interleukin-1β-induced human rheumatoid synovial fibrorlast prostaglandin E_2 formation, J. Biol. Chem. 271 (1996) 31496–31501.

[24] J.A. Cooper Jr., J.M. Parks, R. Carcelen, S.S. Kahlon, M. Sheffield, R. Culbreth, Attenuation of Interleukin-8 production by inhibiting Nuclear Factor-κB translocation using decoy oligonucleotides, Biochem. Pharmacol. 59 (2000) 605–613.

[25] D.C. Hess, E. Howard, C. Cheng, J. Carroll, W.D. Hill, Hypertonic mannitol loading NF-κB transcription factor decoys in human brain microvascular endothelial cells blocks upregulation of ICAM-1, Stroke 31 (2000) 1179–1186.

[26] S.L. Loke, C.A. Stein, X.H. Zhang, K. Mori, M. Nakanishi, C. Subasinghe, J.S. Cohen, L.M. Neckers, Characterization of oligonucleotide transport into living cells, Proc. Natl. Acad. Sci. U. S. A. 86 (1989) 3474–3478.

[27] L.A. Yakubov, E.A. Deeva, V.F. Zarytova, E.M. Ivanova, A.S. Ryte, L.V. Yurchenko, V.V. Vlassov, Mechanism of oligonucleotide uptake by cells: involvement of specific receptors? Proc. Natl. Acad. Sci. U. S. A. 86 (1989) 6454–6458.

[28] C. Beltinger, H.U. Saragovi, R.M. Smith, L. LeSauteur, N. Shah, L. DeDionisio, L. Christensen, A. Raible, L. Jarett, A.M. Gewirtz, Binding, uptake, and intracellular trafficking of phosphorothioate-modified oligodeoxynucleotides, J. Clin. Invest. 95 (1995) 1814–1823.

[29] S. Akhtar, R.L. Juliano, Cellular uptake and intracellular fate of antisense oligonucleotides, Trends Cell Biol. 2 (1992) 139–144.

[30] S. Kawakami, F. Yamashita, K. Nishida, J. Nakamura, M. Hashida, Glycosylated cationic liposomes for cell-selective gene delivery, Crit. Rev. Ther. Drug Carr. Syst. 19 (2002) 171–190.

[31] S. Kawakami, A. Sato, M. Nishikawa, F. Yamashita, M. Hashida, Mannose receptor-mediated gene transfer into macrophages using novel mannosylated cationic liposomes, Gene Ther. 7 (2000) 292–299.

[32] S. Kawakami, S. Fumoto, M. Nishikawa, F. Yamashita, M. Hashida, In vivo gene delivery to the liver using novel galactosylated cationic liposomes, Pharm. Res. 17 (2000) 306–313.

[33] S. Fumoto, S. Kawakami, Y. Ito, K. Shigeta, F. Yamashita, M. Hashida, Enhanced hepatocyte-selective in vivo gene expression by stabilized galactosylated liposome/plasmid DNA complex using sodium chloride for complex formation, Mol. Ther. 10 (2004) 719–729.

[34] S. Kawakami, Y. Hattori, Y. Lu, Y. Higuchi, F. Yamashita, M. Hashida, Effect of cationic charge on receptor-mediated transfection using mannosylated cationic liposome/plasmid DNA complexes following the intravenous administration in mice, Pharmazie 59 (2004) 405–408.

Biodistribution Characteristics of All-*trans* Retinoic Acid Incorporated in Liposomes and Polymeric Micelles Following Intravenous Administration

SHIGERU KAWAKAMI,[1] PRANEET OPANASOPIT,[2] MASAYUKI YOKOYAMA,[3] NARIN CHANSRI,[1] TATSUHIRO YAMAMOTO,[3] TERUO OKANO,[2] FUMIYOSHI YAMASHITA,[1] MITSURU HASHIDA[1]

[1]Department of Drug Delivery Research, Graduate School of Pharmaceutical Sciences, Kyoto University, Sakyo-ku, Kyoto 606-8501, Japan

[2]Institute of Biomedical Engineering, Tokyo Women's Medical University, 8-1 Kawada-cho, Shinjuku-ku, Tokyo 162-8666, Japan

[3]Kanagawa Academy of Science and Technology, KSP East 404, Sakado 3-2-1, Takatsu-ku, Kawasaki-shi, Kanagawa, 213-0012, Japan

Received 14 April 2005; revised 9 June 2005; accepted 23 June 2005

Published online 28 October 2005 in Wiley InterScience (www.interscience.wiley.com). DOI 10.1002/jps.20487

ABSTRACT: The aim of this study was to investigate the biodistribution characteristics of all-*trans* retinoic acid (ATRA) incorporated in liposomes and polymeric micelles following intravenous administration. [^{3}H] ATRA were incorporated in distearoylphosphatidylcholine (DSPC)/cholesterol (6:4) liposomes. Two types of block copolymers, poly (ethylene glycol)-b-poly-(aspartic acid) derivatives with benzyl (Bz-75) groups, were synthesized to prepare the polymeric micelles for [^{3}H]ATRA incorporation. ATRA were dissolved in mouse serum to analyze their inherent distribution. After intravenous administration, the blood concentration of [^{3}H] ATRA in liposomes and polymeric micelles (Bz-75) was higher than that of inherent [^{3}H]ATRA, suggesting that liposomes and polymeric micelles (Bz-75) control the distribution of ATRA. Pharmacokinetic analysis demonstrated that [^{3}H]ATRA incorporated in polymeric micelles (Bz-75) exhibit the largest AUC_{blood} and lowest hepatic clearance of ATRA, suggesting that polymeric micelles (Bz-75) are an effective ATRA carrier system for acute promyelocytic leukemia (APL) therapy. These results have potential implications for the design of ATRA carriers for APL patients. © 2005 Wiley-Liss, Inc. and the American Pharmacists Association J Pharm Sci 94:2606–2615, 2005

Keywords: controlled delivery; controlled release; liposomes; nanoparticles; polymeric drug delivery systems; all-*trans* retinoic acid; polymeric micelle

INTRODUCTION

Retinoids can be natural or synthetic analogs of vitamin A and they normally play a critical role in growth, vision, reproduction, differentiation, and immune function. Recently, it has been demonstrated that all-*trans* retinoic acid (ATRA) is an extremely effective retinoid against acute promyelocytic leukemia (APL) when administered orally in clinical trials.[1,2] However, a gradual decrease in the blood ATRA concentration was observed after continuous oral administration and many patients relapsed after a short period of remission.[3–5] These lower levels are unable to sustain the differentiation effects on leukemic cells *in vivo*, leading to a relapse of the disease and retinoid resistance.[6]

To improve the potency and duration of ATRA activity, liposome[6–8] or emulsion[9,10] formulations

Correspondence to: Mitsuru Hashida (Telephone: 81-75-753-4525; Fax: 81-75-753-4575; E-mail: hashidam@pharm.kyoto-u.ac.jp)

Journal of Pharmaceutical Sciences, Vol. 94, 2606–2615 (2005)

are currently being developed for intravenous administration because of the lower water solubility of ATRA. In particular, clinical trials have demonstrated that liposomal ATRA offers potential pharmacological advantages over the oral administration of ATRA. Estey et al.[6] reported that serum ATRA concentrations were higher and could be maintained longer after ATRA was incorporated in liposomes than after oral administration of ATRA. Thus, liposomes are an effective carrier of ATRA for APL therapy.

Since sustained retention of ATRA in blood could enhance its pharmacological effect, a novel drug carrier system should be developed for optimum APL therapy. It has been reported that the polymeric micelles formed from block copolymers, which are tandem rows of two kinds of polymer chain (A and B), are very stable in the blood circulation because they prevent RES uptake.[11–13] The highly hydrated outer PEG shells of the polymeric micelles can inhibit intermicellar aggregation of their hydrophobic inner cores. Polymeric micelles maintain a satisfactory aqueous stability irrespective of the high content of hydrophobic drug incorporated within the micelle inner core. Therefore, polymeric micelles are expected to be a more effective carrier of ATRA.

The hydrophobic inner core will play a very important role in the stable incorporation of ATRA in polymeric micelles because hydrophobic ATRA is trapped in this inner core. We have succeeded in synthesizing various AB-type block copolymers by varying the chemical structure of the hydrophobic segment of poly(ethylene glycol)-poly(aspartate) block copolymers.[14,15] Because ATRA is a hydrophobic drug, block copolymer, poly(ethylene glycol)-poly(benzyl aspartate) (PEG-P(Asp(Bz))), which is introduced by a hydrophobic chain was synthesized (Scheme 1), and ATRA were incorporated in the polymeric micelles prepared from these block copolymers.

In order to achieve a rational design of the carrier for ATRA, the distribution characteristics

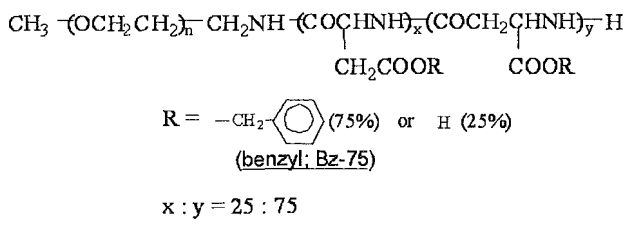

Scheme 1. Chemical structure of block copolymer with benzyl groups.

of ATRA, with or without the carrier (liposome or polymeric micelles), need to be clarified. In the present study, the biodistribution characteristics of [^{3}H]ATRA incorporated in liposomes and polymeric micelles (Bz-75) was investigated after intravenous administration. Because of the lower water solubility of ATRA, it was dissolved in serum to analyze its inherent distribution[16,17] [^{3}H] Cholesteryl hexadecyl ether (CHE), which is a cholesterol derivative, was selected as a liposome tracer because of its high lipophilicity.[18,19]

MATERIALS AND METHODS

Materials

Soluene 350 was purchased from Packard (Groningen, Netherlands). ATRA was purchased from Wako Pure Chemicals Industry Ltd. (Osaka, Japan). Distearoylphosphatidylcholine (DSPC) and cholesterol (Chol) was purchased from Sigma Chemical Co., (St. Louis, MO) and Nacalai Tesque Inc. (Kyoto, Japan), respectively. [^{3}H]ATRA was purchased from NEN Life Science Products, Inc., (Boston, MA). All other chemicals were of the highest purity available.

Preparation of ATRA Incorporated in Liposomes

The DSPC:cholesterol (6:4 molar ratio) was prepared as the control liposome based on the results of published studies.[20] Briefly, the mixtures together with ATRA were first dissolved in chloroform. After vacuum drying and desiccation, pH 7.4 phosphate-buffered saline was added for hydration at 30 min. Radiolabeling of the liposomes was carried out by the addition of [^{3}H]CHE or [^{3}H]ATRA (50 μCi) to the lipid mixture before formation of a thin film layer. The suspension was sonicated for 3 min (200 W) at 4°C using ultrasonic sonicator (US 300, Nissei, Inc., Tokyo, Japan) and the resulting liposomes were extruded through 200-nm (five times) and 100-nm (five times) polycarbonate membrane filters using an extruder device preheated to 60°C. The filtered ATRA was adjusted to a concentration of 0.06 mg/mL based on the measured radioactivity. The particle size of the liposomes was measured in a dynamic light scattering spectrophotometer (LS-900, Otsuka Electronics, Osaka, Japan).

Synthesis of Block Copolymer with Benzyl Group

The chemical structure of a block copolymer used for incorporation of ATRA into polymeric micelles

with benzyl group is shown in Scheme 1. This is a poly(ethylene glycol)-b-poly(aspartic acid) derivative block copolymer.[15] The molecular weight of the poly(ethylene glycol) (PEG) chain was 5000 and the average number (x + y) of the aspartic acid units was 27. Approximately 75% of the aspartic acid residues of the poly(aspartic acid) chain were converted to the β-amide form due to an alkaline hydrolysis procedure during the synthesis of this block copolymer. A hydrophobic benzyl group was bound to 75% of the poly(aspartic acid) residues by an ester-forming reaction between benzyl bromide and poly(ethylene glycol)-poly(aspartic acid) block copolymer (PEG-P(Asp)) as reported previously.[21] Briefly, PEG-P (Asp) block copolymer was dissolved in *N,N*-dimethylformamide (DMF) and added to benzyl bromide along with a catalyst, 1, 8-diazabicyclo[5,4,0]7-undecene (DBU). The reaction mixture was stirred at 50°C for 15.5 h. Polymers were obtained by precipitation in an excess of diethyl ether and collected by centrifugation at 3000 rpm for 10 min. The dried polymer was dissolved in dimethyl sulfoxide (DMSO) and added to an excess of 6 N HCl, followed by dialysis against distilled water and, finally, freeze-drying.

For determination of the polymer composition, such as the number of Asp units and the benzyl ester content, ^{1}H-NMR measurements were carried out on a 1% solution in 6D-DMSO containing 3% trifluoroacetic acid using a Varian Unity Inova NMR spectrometer at 400 MHz.

Incorporation of ATRA into Polymeric Micelles

Incorporation of ATRA into polymeric micelles was carried out by an evaporation method. Briefly, ATRA 0.5 mg and polymer 5 mg were dissolved in chloroform. After vacuum drying and desiccation, 3 mL of phosphate buffered saline (pH 7.4) was added for hydration for 30 min at 25°C. The preparation was placed in a probe sonicator (200 W) for 2 min at 4°C. The obtained preparation was centrifuged at 1500*g* for 10 min before the supernatant was passed through a 0.45 μm filter. To prepare [^{3}H]ATRA-labeled polymeric micelles, a trace amount of [^{3}H] ATRA (50 μCi) was dissolved in chloroform with ATRA and polymer and then treated exactly as described above. The filtered ATRA was adjusted to a concentration of 0.06 mg/mL based on the measured radioactivity.

Incorporation of ATRA in the polymeric micelles was confirmed by gel-permeation chromatography in distilled water. ATRA was found to elute at the gel-exclusion volume of a Tosoh TSKgel G3000PW$_{XL}$ column (exclusion molecular weight = 500000) using a UV detector operated at 360 nm. This indicates that ATRA was incorporated into polymeric micelles having a molecular weight of 500000 or more. The amount of incorporated ATRA in the polymeric micelles was determined by the UV absorption at 360 nm of the micelle solution in a mixture of dimethylsulfoxide (DMSO) and water (DMSO: water = 9: 1 by volume). The filtered ATRA was adjusted to a concentration of 0.06 mg/mL based on the measured radioactivity. The particle size of the polymeric micelles was measured in a dynamic light scattering spectrophotometer (LS-900, Otsuka Electronics).

Evaluation of ATRA Incorporated in Polymeric Micelles

The methods used to determine the incorporation ratio of ATRA in polymeric micelles were as described for the liposomal studies.[22] Briefly, the polymeric micelles were ultrafiltered using a micropartition system (Sartorion VIVASPIN 2 mL concentrator 5000 MWCO PES) at 1500*g* for 15 min. The drug concentration in the preparation (C_T) and in the ultrafiltrate (C_W) was assayed by scintillation counting. The equation for the incorporation ratio in the polymeric micelles was as follows:

$$\text{Incorporation ratio (\%)} = ((C_T - C_W)/C_T) \times 100$$

Preparation of Mouse Serum

Mice were prepared according to the method reported previously.[16,17] Mouse blood was collected and coagulated by incubation for 12 h. After centrifugation (1500*g*) for 10 min, the supernatant was filtered (0.45 μm).

In Vivo Distribution Study

Five-week-old male ddY mice (25.0–27.0 g) were obtained from Shizuoka Agricultural Co-operative Association for Laboratory Animals, Shizuoka, Japan. [^{3}H]ATRA (0.5 μCi/100 μl) dissolved in serum, polymeric micelles or liposomes were injected into the tail vein of mice at a ATRA dose of 0.6 mg/kg. At each collection time point, blood was collected from the vena cava and the mice were then killed at the end of the experiment. The

liver, kidneys, spleen, heart, and lungs were removed, washed with saline, blotted dry, and weighed. Ten microliters of blood and precisely weighed a small amount of each tissue (20–30 mg) were digested in 0.7 mL Soluene-350 by incubating overnight at 45°C. Following digestion, 0.2 mL isopropanol, 0.2 mL 30% hydroperoxide, 0.1 mL 5 N HCl, and 5.0 mL Clear-Sol I were added. The samples were stored overnight and the radioactivity was measured in a scintillation counter (LSA-500, Beckman, Tokyo, Japan).

Calculation of Organ Clearance

The tissue distribution data were evaluated using organ distribution clearances as reported previously.[23,24] Briefly, the tissue uptake rate can be described by the following equation

$$\frac{dX_t}{dt} = CL_{uptake} \cdot C_b \quad (1)$$

where X_t is the amount of [^{3}H] ATRA in the tissue at time t, CL_{uptake} is the tissue uptake clearance, and C_b is the blood concentration of [^{3}H] ATRA. Integration of Equation 1 gives

$$X_t = CL_{uptake} \cdot AUC_{(0\sim t)} \quad (2)$$

where $AUC_{(0\sim t)}$ represents the area under the blood concentration time curve from time 0 to t. The CL_{uptake} value can be obtained from the initial slope of a plot of X_t versus $AUC_{(0\sim t)}$.

In Vitro Penetration Study

The dialysis membranes (Spectra/Por® Membrane MWCO 3,500, Spectrum Laboratories, Inc., Roncho Dominguez, CA) were mounted in diffusion chambers. Then, 2.2 mL phosphate buffered saline (pH 7.4) or 20% DMSO phosphate buffered saline (pH 7.4) (DMSO: phosphate buffered saline (pH 7.4) = 8: 2 by volume) was added to the donor and receiver side. The diffusion chambers were maintained at 37°C and 0.8 mL of ATRA (140 μM) incorporated in polymeric micelles were added to the donor side (initial donor concentration (C_I) = 37.3 μM). At 3, 12, and 20 h, samples (40 μl) were withdrawn from receiver side and the penetration concentrations of ATRA (C_P) were determined spectrophotometer (UV-visible Spectrophotometer, Shimazu Co., Ltd., Kyoto, Japan; 350 nm). The equation for the penetration % was as follows:

$$\text{Penetration } (\%) = (C_P/C_I) \times 100$$

Statistical Analysis

Statistical comparisons were performed by Student's t-test for two groups, and one-way ANOVA for multiple groups. $p < 0.05$ was considered to be indicative of statistical significance.

RESULTS

Mean Diameter of ATRA Incorporated in Liposomes or Polymeric Micelles

The particle size distribution of ATRA incorporated in liposomes and polymeric micelles was analyzed. The weight-fractioned mean diameter of sonicated samples of liposomes and polymeric micelles (Bz-75) were about 113 and 19.1 nm. These sizes of ATRA incorporated in liposomes and polymeric micelles corresponded to our previous observations for each formulation.

Incorporation Ratio of ATRA in Liposomes or Polymeric Micelles

The incorporation ratio of ATRA in liposomes and polymeric micelles was 95.6 ± 0.42 ($n = 3$) and 96.4 ± 0.17 % ($n = 3$), indicating that most of the ATRA was tightly incorporated in the liposomes and the polymeric micelles (Bz-75).

Blood Concentration of [^{3}H]ATRA or [^{3}H]CHE Incorporated in Liposomes

Figure 1 shows the blood concentration profiles of [^{3}H]ATRA dispersed in serum (inherent distribution of ATRA) and [^{3}H]ATRA or [^{3}H]CHE incorporated in polymeric micelles or liposomes after intravenous injection into mice. The blood concentration of [^{3}H] ATRA in mouse serum was significantly lower than that of [^{3}H] ATRA in liposomes, suggesting that liposomes could enhance blood retention by their encapsulation. However, the blood concentration of [^{3}H] ATRA in liposomes was significantly lower than that of [^{3}H] CHE in liposomes. Taking the incorporation percentage of ATRA in liposomes (96.4%) into considerations, most of the ATRA is rapidly released in the blood circulation after intravenous injection.

Blood Concentration of [^{3}H]ATRA Incorporated in Polymeric Micelles

Scheme 1 shows the structure of the block copolymer used to prepare the polymeric micelles.